Mathematical Modeling of Coupled Electro-thermal Response of Nerve Tissues Subjected to Radiofrequency Fields

Singh, S. and Melnik, R.

In: D. M. Kilgour et al. (eds.), Recent Developments in Mathematical, Statistical and Computational Sciences, Springer Proceedings in Mathematics & Statistics 343, 10 pages, 2021,
Springer Nature, Switzerland.

Mathematical Modeling of Coupled Electro-thermal Response of Nerve Tissues Subjected to Radiofrequency Fields

Sundeep Singh and Roderick Melnik

Abstract This study aims at developing a mathematical model taking into account the effects of thermal pain sensation induced during the radiofrequency heating of neural tissues. A three-dimensional heterogeneous computational domain comprising of muscle, bone and target nerve has been considered. Importantly, the main governing equations of the multi-scale and multi-physics model are: (a) a simplified version of Maxwell's equation utilizing a quasi-static approximation for estimating the electric field distribution, (b) the Pennes bioheat transfer equation for estimating the temperature distribution and (c) a modified Hodgkin-Huxley model for prediction of nociceptor electrophysiology. The temperature-controlled radiofrequency has been modeled on the neural tissue by utilizing the protocols applied in actual clinical practices along with taking into account the temperature-dependent electrical conductivity and blood perfusion rate. The effects of different values of preset target temperature on the treatment outcomes of nerve ablation have also been quantified. The findings of the present study would provide *a priori* information to the clinicians that will be beneficial during the treatment planning stage of the therapy.

1 Introduction

Chronic pain is one of the most common problems affecting millions of Canadians each year and contributes to the significant burden on healthcare resources ($\approx$ \$7.2 billion annually) [1]. The management of chronic pain is largely based on the use of

Sundeep Singh
MS2Discovery Interdisciplinary Research Institute, Wilfrid Laurier University, 75 University Avenue West, Waterloo, Ontario, N2L 3C5, Canada, e-mail: ssingh@wlu.ca

Roderick Melnik
MS2Discovery Interdisciplinary Research Institute, Wilfrid Laurier University, 75 University Avenue West, Waterloo, Ontario, N2L 3C5, Canada, e-mail: rmelnik@wlu.ca
BCAM – Basque Center for Applied Mathematics, E-48009 Bilbao, Spain

opioids medication, misuse of which could lead to negative effects such as physical dependence and addiction [1, 2]. There has been a continuous quest for exploring treatment options that are cheap and effective for long durations, and could minimize the need for opioids. Radiofrequency ablation is one such treatment options that has been frequently applied in the last decade for the management of different types of chronic pain [3, 4]. The setup of the minimally invasive radiofrequency (RF) procedure comprises of the RF generator, the dispersive ground pad and an electrode with a small portion of the active length. Once the electrode is placed at the target site, alternating current within the kHz range is delivered from the RF generator to the target nerve via the active part of the electrode that is further captured and returned back to the generator by the ground pad, forming a closed electric circuit. As the RF current interacts with the biological tissue, frictional heating is induced due to the agitation of ions present within the tissue electrolytes [2, 4]. By virtue of this, temperatures above 50 °C are achieved close to the active site of the electrode leading to biological changes such as protein and collagen denaturation and ultimately coagulative necrosis. The attainment of high temperature (close to 100 °C) during the RF procedure could further lead to side effects such as tissue charring and vaporization, and is often an indication to stop the RF procedure as it results in a drastic decline in electrical and thermal conductivities of the tissue, thereby acting as a barrier to the efficient conduction of thermal energy [3]. In general, the RF power is delivered to the neural tissue using different modes, viz., continuous and pulsed. In the conventional continuous mode, the RF power is delivered to the target neural tissue in a continuous manner, leading to the destruction of the axons and limiting the transmission of pain signals. While, in the pulsed RF mode, short pulses of RF currents are applied to the target nerve that allows heat to dissipate and restricts the attainment of temperatures above 42 °C during the entire procedure, thereby avoiding any thermal damage [2, 4].

Although the usage of RF procedure for mitigating chronic pain has been increasing tremendously during the past decades, several questions and controversies still prevail regarding the underlying mechanism, efficacy and benefits of RF [1, 2, 4]. Computational modeling can provide a cheap and viable alternative for quantifying the underlying physics and providing *a priori* estimate of the treatment outcomes that could assist the clinicians in optimizing and standardizing the treatment protocols specific to particular target sites of neural tissues. In what follows, the present study focuses on developing more realistic three-dimensional heterogeneous models of continuous RF for treating chronic pain. A temperature-controlled algorithm has been used whereby the maximum temperature during the RF procedure won't be allowed to reach 100 °C to mitigate any chances of occurrence of undesirable phenomena of charring and water vaporization. The effect of preset target temperature on the applied voltage, temperature distribution and ablation volume has been quantified by conducting a coupled thermo-electric analysis. Furthermore, the rise in tissue temperature during RF procedure could also lead to the induction of nociceptive pain other than the target site and mainly close to the skin tissue. Importantly, the transduction of nociceptive pain occurs through the nociceptors that reside at the ends of the long axons of neurons and mediate the selective passage of specific

ions or molecules across cell membranes at noxious temperature levels. The nociceptors are one of the three kinds of peripheral nerves: myelinated afferent $A\delta$ and $A\alpha$ fibers, and unmyelinated C afferent fibers. Thermal pain sensations are mainly mediated by both myelinated $A\delta$ and unmyelinated C fibers [5, 6]. Thus, the effect of such nociception has also been taken into consideration within the computational model of the temperature-controlled RF procedure.

2 Computational Modeling Details

The schematic of a three-dimensional heterogeneous computational domain comprising of muscle, bone and nerve tissue [7] considered in the present numerical study has been presented in Fig. 1. A 22-gauge (5 mm active length) monopolar RF electrode [8] has been inserted parallel to the target nerve, as shown in Fig. 1. The temperature-controlled RF procedure has been performed by utilizing a closed-loop feedback proportional-derivative-integral (PID) controller that continuously modulates the applied voltage at the active length of the electrode on the basis of the difference between the preset target temperature and the predicted temperature at the tip of the RF electrode [9, 10]. Three different values of preset target tip temperatures, viz., 65 °C, 75 °C and 85 °C have been considered. The dispersive ground electrode has been modeled by applying zero voltage boundary conditions at the outer boundaries of the computational domain. The initial voltage of the computational domain has been considered to be 0 V and the initial temperature has been considered similar to the core body temperature of 37 °C. The material properties considered in the present study are provided in Table 1 [3, 7, 8, 11, 12].

The computational model considered in this study is based on the coupled thermo-electric problem where electromagnetic energy is used to heat the neural

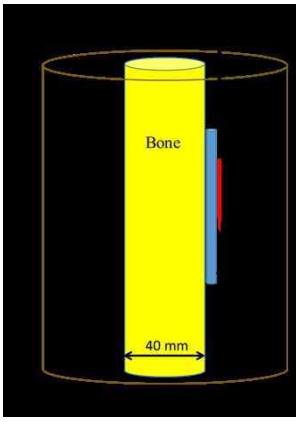

Fig. 1 (Color online) Schematic of a three-dimensional heterogeneous computational domain comprising of nerve, bone and muscle tissue along with monopolar RF electrode.

Table 1 Electric, thermal and biophysical properties of different materials considered in this study.

Material	σ (S/m)	c (J/kg/K)	k (W/m/K)	ρ (kg/m^3)	ω_b (s^{-1})
Muscle	0.446	3421	0.49	1090	6.35×10^{-4}
Bone	0.0222	1313	0.32	1908	4.67×10^{-4}
Nerve	0.111	3613	0.49	1075	3.38×10^{-3}
Plastic	10^{-5}	1045	0.026	70	–
Electrode	7.4×10^6	480	15	8000	–

tissue during continuous RF procedure for treating chronic pain. Due to the lower frequency range of 450-550 kHz used during the RF procedures, the wavelength of the electromagnetic field is several orders of magnitude larger than the size of the active electrode. Thus, a simplified version of Maxwell's equations, known as the quasi-static approximation, can be used to solve the electromagnetic problem without compromising accuracy [3, 7, 8, 9, 10, 11, 12]. The governing equation for the electrical problem is given by:

$$\nabla \cdot (\sigma(T)\nabla V) = 0, \tag{1}$$

where σ (+2 % per °C) is the temperature-dependent electrical conductivity (S/m) [9] and V is the applied voltage (V). Further, the volumetric heat source, Q_p (W/m^3), generated by RF currents within the biological tissue is given by:

$$Q_p = \mathbf{J} \cdot \mathbf{E}, \tag{2}$$

where $\mathbf{E} = -\nabla$V (in V/m) is the electric field and $\mathbf{J} = \sigma(T)\mathbf{E}$ (in A/m^2) is the current density.

The governing equation for the thermal problem is the Fourier-conduction-based Pennes bioheat transfer equation and is given by:

$$\rho c \frac{\partial T}{\partial t} = \nabla \cdot (k \nabla T) - \rho_b \, c_b \omega_b \, (T - T_b) + Q_m + Q_p, \tag{3}$$

where ρ is the density (kg/m^3), c is the specific heat capacity (J/kg/K), k is the thermal conductivity (W/m/K), ρ_b is the density of blood (3617 kg/m^3), c_b is the specific heat capacity of blood (1050 J/kg/K), ω_b is the blood perfusion rate (1/s) i.e. volume blood per unit mass of tissue per unit time, T_b is the blood temperature (37 °C), T is the unknown temperature of the tissue to be computed from Equation 3, Q_p is the volumetric heat source (W/m^3) computed using Equation 2, Q_m is the metabolic heat generation (W/m^3) that has been neglected in the present study [8] due to its insignificant contribution as compared to Q_p and t is the duration of the temperature-controlled RF procedure (s).

In the present computational study, a temperature-dependent piecewise model of blood perfusion rate has been considered. Accordingly, a constant predefined value of blood perfusion rate has been assumed below the tissue temperature of

50 °C and beyond that, the value of blood perfusion rate has been considered to be zero owing to the complete cessation of blood perfusion rate due to the collapse of microvasculature within the tissue [13] and is given by:

$$\omega_b(T) = \left\{ \begin{array}{c} \omega_{b,0} \text{ for } T < 50\,^{\circ}C \\ 0 \quad \text{for } T \geq 50\,^{\circ}C \end{array} \right\}, \tag{4}$$

where $\omega_{b,0}$ is the constant blood perfusion rate of tissue provided in Table 1.

The ablation volume ($\dot{V}$) induced during the temperature-controlled RF procedure for chronic pain relief has been quantified using the isotherm of 50 °C (i.e. the volume of tissue within the computational domain having temperature $\geq 50\,^{\circ}$C after the RF procedure) [13] and is given by:

$$\dot{V} = \iiint_{\Omega} dV\,(\text{mm}^3) \quad (\text{where } \Omega \geq 50^0 C). \tag{5}$$

A modified Hodgkin-Huxley model has been used for modeling the nociceptor signal transduction induced due to the high temperature attained during the RF procedure close to the skin surface. It is given by [5, 6]:

$$C_{mem}\frac{dV_{mem}}{dt} = I_{st} + I_{Na} + I_K + I_{K2} + I_L, \tag{6}$$

where V_{mem} is the membrane potential (mV) that is positive for depolarized membrane and negative for hyperpolarized membrane, t is the neuronal discharge time (ms), C_{mem} is the membrane capacitance per unit area (μA/cm^2). I_{Na}, I_K and I_L are the sodium, potassium and transmembrane leakage currents (all in μA/cm^2), respectively, while I_{K2} is the fast transient potassium current. They are computed as follows:

$$I_{Na} = g_{Na}m^3h\,(V_{Na} - V_{mem}); \quad I_K = g_K n^4\,(V_K - V_{mem}), \tag{7}$$

$$I_L = g_L\,(V_L - V_{mem}); \quad I_{K2} = g_A A^3 B\,(V_{K2} - V_{mem}), \tag{8}$$

where V_{Na}, V_K, V_L and V_{K2} are the corresponding reversal potentials (in mV) for the sodium, potassium, leakage and fast transient sodium currents, respectively, g_{Na}, g_K, g_L and g_{K2} (in mS/cm^2) are the maximum ionic conductances per unit area through the sodium, potassium, leakage and fast transient sodium current components, respectively; m, n and h are the gating variables, and A and B are factors having the same functional significance as factors m and h. $I_{st} = I_{mechanical} + I_{heat} + I_{chemical}$ is the total stimulation induced current (in μA/cm^2) that can be computed as the sum of the currents generated due to the opening of mechanically-, thermally- and chemically-gated ion channels, respectively. Since in this study only the thermal stimulation was applied on the axons, thus only thermally-gated ion channels were considered for the generation of stimulation current [6] and is given by:

$$I_{st} = I_{heat} = \left(\left[C_{h1} \exp\left(\frac{(T - T_{thr})/T_{thr}}{C_{h2}} \right) + C_{h3} \right] + I_{shift} \right) \cdot H(T - T_{thr}), \tag{9}$$

where T is the temperature experienced by nociceptors, T_{thr} is the thermal pain threshold temperature, C_{h1}, C_{h2} and C_{h3} are constants and I_{shift} is the shift current that ensures that the action potential is generated when $T \geq T_{thr}$ while none is generated if $T < T_{thr}$. H is the Heaviside function accounting for the threshold process. The gating variables: m, n and h can be computed from the following equations [6]:

$$\frac{\mathrm{d}x}{\mathrm{d}t} = \alpha_x (1-x) - \beta_x x, \tag{10}$$

$$\alpha_n = -0.01\,(V_{mem}+50)/(\exp[-(V_{mem}+50)/10\,]-1), \tag{11}$$

$$\alpha_m = -0.1\,(V_{mem}+35)/(\exp[-(V_{mem}+35)/10\,]-1), \tag{12}$$

$$\beta_n = 0.125\exp[-(V_{mem}+60)/80\,];\ \beta_m = 4\exp[-(V_{mem}+60)/18\,], \tag{13}$$

$$\alpha_h = 0.07\exp[-(V_{mem}+60)/20\,];\ \beta_h = 1/(\exp[-(V_{mem}+30)/10\,]+1), \tag{14}$$

where x is one of the three gating variables (m, n or h), α_x and β_x are the rate constants (s^{-1}) determined from the voltage clamp experiments [6]. Further, the factors A and B are determined from the following sets of equations [6]:

$$\tau_A \frac{\mathrm{d}A}{\mathrm{d}t} + A = A_\infty, \tag{15}$$

$$A_\infty = \left(0.0761\,\frac{\exp[(V_{mem}+94.22)/31.84\,]}{1+\exp[(V_{mem}+1.17)/28.93\,]}\right)^{1/3}, \tag{16}$$

$$\tau_A = A_{fac}\left(0.3632 + \frac{1.158}{1+\exp[(V_{mem}+55.96)/20.12\,]}\right), \tag{17}$$

$$\tau_B \frac{\mathrm{d}B}{\mathrm{d}t} + B = B_\infty, \tag{18}$$

$$B_\infty = \left(\frac{1}{1+\exp[(V_{mem}+53.3)/14.54\,]}\right)^4, \tag{19}$$

$$\tau_B = B_{fac}\left(1.24 + \frac{2.678}{1+\exp[(V_{mem}+50)/16.03]}\right). \tag{20}$$

Motivated by [6], the values of different parameters used in the nociception model are: C_{mem} = 2.8 μF/cm^2, g_{K2} = 47.7 mS/cm^2, g_{Na} = 120 mS/cm^2, g_K = 36 mS/cm^2, g_L = 0.3 mS/cm^2, $A_{fac} = B_{fac}$ = 7.0, V_{Na} = 57.19 mV, V_K = -78.78 mV, V_L = -63.79 mV, $C_{h1} = C_{h2}$ = 2, C_{h3} = -1 μA/cm^2, T_{thr} = 43 °C and V_{rest} = -70 mV.

The coupled thermo-electric models of temperature-controlled RF procedure for treating chronic pain have been solved by the Finite Element Method (FEM) using COMSOL Multiphysics 5.2 software [14] utilizing an adaptive time-stepping scheme. The computational domain has been discretized using heterogeneous tetrahedral mesh, comprising of 174486 elements and 476384 degrees of freedom, constructed with COMSOL's built-in mesh generator. A further refinement in the area surrounding the active tip of the electrode has been applied, where the highest electrical and thermal gradients are expected. A mesh convergence analysis has been carried out to determine the optimal number of mesh elements that would result in a mesh-independent solution. The temperature distribution computed from the coupled thermo-electric model was fed in the MATLAB code of the modified Hodgkin Huxley model for predicting the nociceptor response to these predicted temperatures. All simulations were run on a Dell T7400 workstation with Quad-core 2.0 GHz Intel® Xeon® processors.

3 Results and Discussion

The effect of different values of preset target temperature, viz., 65 °C, 75 °C and 85 °C, on the tip temperature and the applied voltage during the temperature-controlled RF procedure has been presented in Fig. 2. As it is evident from Fig. 2, initially, the applied voltage value increases monotonically till the preset target temperature has been attained and afterward it declines to maintain the preset value of target temperature. This is true for all values of preset target temperature considered in this numerical study, although the rise in the values of preset target temperature results in the corresponding rise in the applied voltage profile. This can be attributed to the requirement of more energy for attaining the higher target temperature value in comparison to attaining the lower value of target temperature. The maximum values of applied voltages for the preset target temperature of 65 °C, 75 °C and 85 °C have been found to be 10.66 V, 12.54 V and 14.19 V, respectively. Furthermore, the time required to attain the preset temperature of 65 °C, 75 °C and 85 °C has been found to be 66 s, 57 s and 51 s, respectively. The variation of target tip temperature follows a similar trends to that of applied voltage, whereby the temperature rises from the core body temperature of 37 °C, i.e. the initial temperature within the computational domain, to the preset value of target tip temperature with an overshoot of ± 5 % which is common in clinical procedures.

Figure 3 presents the comparative analysis of the total ablation volume (within the entire computational domain) and nerve ablation volume corresponding to the isotherm of 50 °C for different values of the target temperature. The total ablation volume after 120 s of the temperature-controlled RF procedure has been found to be 110.86 mm^3, 222.79 mm^3 and 357.50 mm^3 for the target temperature values of 65 °C, 75 °C and 85 °C, respectively. Similarly, the damage that occurred to the target nerve tissue alone has been found to be 24.16 mm^3, 48.91 mm^3 and 75.48 mm^3 for the above target temperature values, respectively, after 120 s of the temperature-controlled RF procedure. Not only this, the variations have also been found in the time at which the initiation of damage occurs for different values of target temperature that basically decreases with the increase of the target tip temperature. Thus, the efficacy of temperature-controlled RF procedure for treating chronic neural pain is significantly dependent on the preset target temperature.

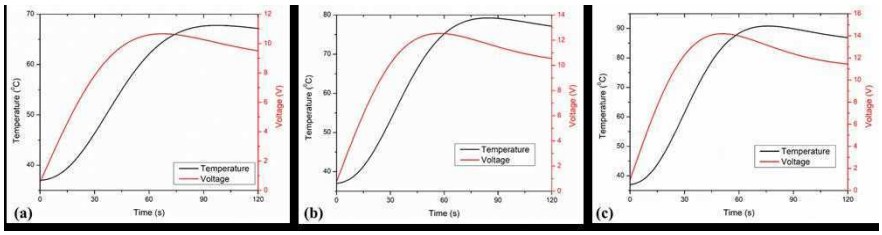

Fig. 2 (Color online) Variation of the applied voltage (red) and tip temperature (black) with respect to time for different values of preset target temperature: (a) 65 °C, (b) 75 °C and (c) 85 °C.

Figure 4 presents the variation of temperature distribution for different preset values of target tip temperature within the computational domain after 120 s of temperature-controlled RF procedure. As depicted in Fig. 4, the attainment of critical temperatures above 50 °C is not only confined to the target nerve, but also to a considerable portion of the healthy muscular tissue on the opposite side of target nerve and bone. The exposure of the muscular tissue just beneath the skin tissue to such higher temperatures could lead to the transduction of nociceptive pain signals through the nociceptors of peripheral nerves (viz., myelinated afferent $A\delta$ and $A\alpha$ fibers; and unmyelinated C afferent fibers) residing at the ends of the long axons of neurons. Thus, the present study also models the effects of such high temperature attained on the healthy muscular tissue during the temperature-controlled RF procedure for chronic pain relief. Figure 5 presents the membrane potential and frequency responses under different values of stimulus temperature, viz., 43 °C, 45 °C and 50 °C. It can be clearly observed from Fig. 5 that the frequency of action poten-

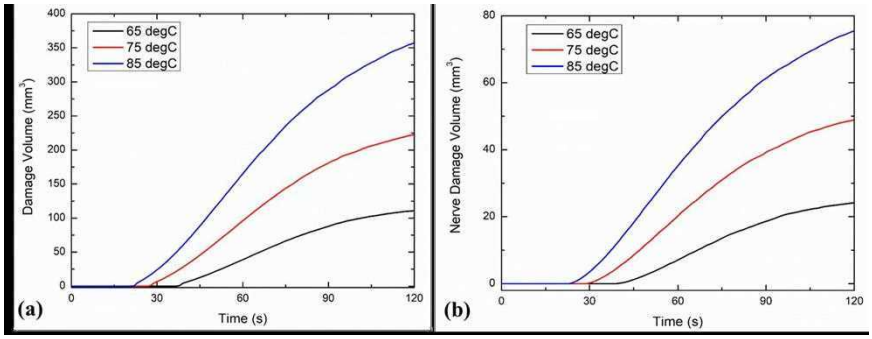

Fig. 3 (Color online) Variation of (a) total damage volume, and (b) nerve damage volume, with respect to time for different values of preset target temperature during the temperature-controlled RF procedure for chronic pain relief (on the insert, black: 65 °C, red: 75 °C, blue: 85 °C).

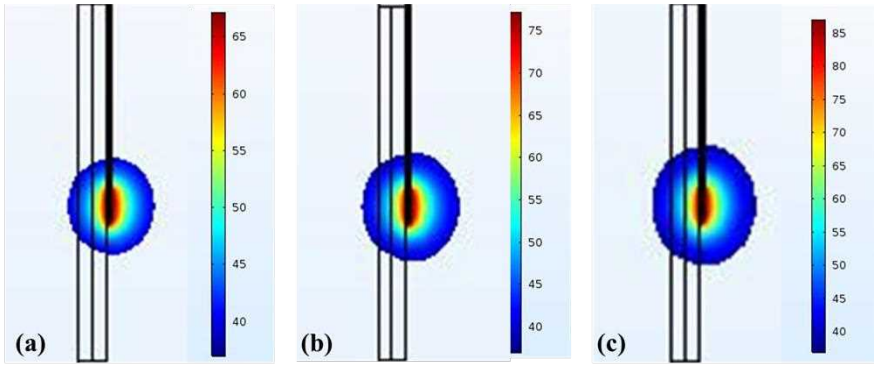

Fig. 4 (Color online) Temperature distribution (in °C) obtained after 120 s of temperature-controlled RF procedure for different values of preset target temperature: (a) 65 °C, (b) 75 °C and (c) 85 °C.

tial spikes increases as the nociceptor temperature increases from 43 °C and 50 °C. The pain level induced due to nociceptor temperature is decided by this signal frequency (i.e. action potential spikes), and thus, the thermal pain level increases as the temperature increases. Such *a priori* estimates about the transduction of nociceptive pain induced due to thermal stimuli would assist the medical practitioners in designing the anesthesia-free thermal ablation procedures for chronic pain relief.

Future studies will be focused on developing fully coupled thermo-electro-neuronal models by taking into consideration the effect of temperature on the membrane conductance in the Hodgkin-Huxley model and non-Fourier heat transfer, along with the incorporation of actual nerve damage models accounting for decrement of the pain signals when exposed to RF procedures [15, 16]. This will enhance the accuracy of the predictive outcomes from the current model that can be readily integrated into the hospital workflow during the real-time treatment of chronic pain among actual patients in clinical settings. Moreover, image-based patient-specific models derived from actual patient data could significantly assist in bridging the gap between computational and experimental findings.

4 Conclusion

A coupled thermo-electric analysis has been performed for quantifying the effect of preset target temperature on the treatment outcomes of the temperature-controlled RF procedure for chronic pain relief. The study reported a strong dependence of the preset target temperature on the efficacy of RF procedure during neural ablation. It has been found that the ablation volume increases with an increase in target tip temperature and vice-versa. Further, a thermo-neuronal model has also been developed to quantify the induction of pain sensation in the nociceptors during such procedures. These predictions could be quite useful in designing the anesthesia-free RF procedure for chronic pain relief. We expect that the advancement and extension of the developed model can significantly assist the clinicians in better optimizing and standardizing the thermal dosages required for enabling safe and reliable RF applications for mitigating chronic pain.

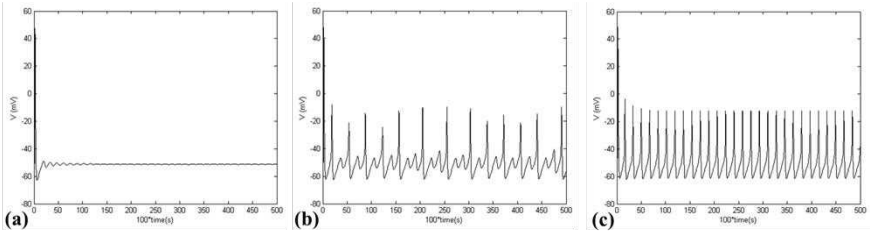

Fig. 5 Predictions of the thermo-neural response of nociceptors at different values of stimulus temperature, viz., (a) 43 °C, (b) 45 °C and (c) 50 °C.

Acknowledgements Authors are grateful to the NSERC and the CRC Program for their support. RM is also acknowledging support of the BERC 2018-2021 program and Spanish Ministry of Science, Innovation and Universities through the Agencia Estatal de Investigacion (AEI) BCAM Severo Ochoa excellence accreditation SEV-2017-0718, and the Basque Government fund AI in BCAM EXP. 2019/00432.

References

1. Loh, E., Reid, J.N., Alibrahim, F., Welk, B.: Retrospective cohort study of healthcare utilization and opioid use following radiofrequency ablation for chronic axial spine pain in Ontario, Canada. Reg. Anesth. Pain. Med. **44**, 398–405 (2019)
2. Deer, T.R., Pope, J.E., Lamer, T.J., Provenzano, D.: Deer's treatment of pain: An illustrated guide for practitioners. Springer, Cham (2019).
3. Singh, S., Melnik, R.: Computational analysis of pulsed radiofrequency ablation in treating chronic pain. In Rodrigues, J., et al. (eds.) Computational Science – ICCS 2019, Lecture Notes in Computer Science, pp. 436-450. Springer, Cham (2019)
4. Soloman, M., Mekhail, M.N., Mekhail, N.: Radiofrequency treatment in chronic pain. Expert Rev. Neurother. **10**(3), 469–474 (2010).
5. Xu, F., Lin, M., Lu, T.J.: Modeling skin thermal pain sensation: role of non-Fourier thermal behavior in transduction process of nociceptor. Comput. Biol. Med. **40**(5), 478–486 (2010)
6. Lin, M., Liu, S., Genin, G., Zhu, Y., Shi, M., Ji, C., Li, A., Lu, T., Xu, F.: Melting away pain: decay of thermal nociceptor transduction during heat-induced irreversible desensitization of ion channels. ACS Biomater. Sci. Eng. **3**(11), 3029–3035 (2017)
7. Singh, S., Melnik, R.: Radiofrequency ablation for treating chronic pain of bones: effects of nerve locations. In Rojas, I., Valenzuela, O., Rojas, F., Ortuño, F. (eds) Bioinformatics and Biomedical Engineering (IWBBIO 2019), Lecture Notes in Computer Science, pp. 418–429, Springer, Cham (2019)
8. Ewertowska, E., Mercadal, B., Muñoz, V., Ivorra, A., Trujillo, M., Berjano, E.: Effect of applied voltage, duration and repetition frequency of RF pulses for pain relief on temperature spikes and electrical field: a computer modelling study. Int. J. Hyperthermia **34**(1), 112–121 (2018)
9. Singh, S., Repaka, R.: Temperature-controlled radiofrequency ablation of different tissues using two-compartment models. Int. J. Hyperthermia **33**(2), 122–134 (2017)
10. Singh, S., Repaka, R.: Numerical study to establish relationship between coagulation volume and target tip temperature during temperature-controlled radiofrequency ablation. Electromagn. Biol. Med. **37**(1), 13–22 (2018)
11. Pérez, J.J., Pérez-Cajaraville, J.J., Muñoz, V., Berjano, E.: Computer modeling of electrical and thermal performance during bipolar pulsed radiofrequency for pain relief. Med. Phys. **41**(7), 071708/11 (2014)
12. Singh, S., Melnik, R.: Domain heterogeneity in radiofrequency therapies for pain relief: A computational study with coupled models. Bioengineering **7**(2), 35 (2020)
13. Singh, S., Repaka, R., Al-Jumaily, A.: Sensitivity analysis of critical parameters affecting the efficacy of microwave ablation using Taguchi method. Int. J. RF Microw. Comput. Aided Eng. **29**(4), e21581 (2019)
14. COMSOL Multiphysics® v. 5.2. www.comsol.com. COMSOL AB, Stockholm
15. Singh, S., Melnik, R.: Thermal ablation of biological tissues in disease treatment: A review of computational models and future directions. Electromagn. Biol. Med. (2020) doi: 10.1080/15368378.2020.1741383
16. Singh, S., Melnik, R.: Coupled thermo-electro-mechanical models for thermal ablation of biological tissues and heat relaxation time effects. Phys. Med. Biol. **64**, 245008 (2019)